PROCEEDINGS OF ECOS 2023 - THE 36TH INTERNATIONAL CONFERENCE ON
EFFICIENCY, **C**OST, **O**PTIMIZATION, **S**IMULATION AND ENVIRONMENTAL IMPACT OF ENERGY SYSTEMS
25-30 JUNE 2023, LAS PALMAS DE GRAN CANARIA, SPAIN

Experimental study of an ultrasonic spray atomiser as an evaporative cooler

Pedro Martínez[a], Javier Ruiz[a], Manuel Lucas[a], Jonás Pérez[a], Pedro Navarro[b] and Alberto Rodríguez[a]

[a] *Miguel Hernández University of Elche, Avda. de la Universidad, s/n, 03202 Elche, Spain, j.ruiz@umh.es, CA*
[b] *Technical University of Cartagena, Dr. Fleming, s/n, 30202 Cartagena, Spain*

Abstract:

The use of evaporative cooling techniques for pre-cooling the inlet air of a condenser used in air conditioning applications has proven to be very effective in improving its performance. Ultrasonic techniques constitute a promising alternative to improve the design of evaporative pre-cooling systems. Compared to direct spray cooling applications, not only they eliminate the pressure loss induced in the inlet air stream but also, they are capable of generating smaller droplet sizes with reduced power consumption than a high-pressure spray nozzle. This paper deals with an experimental investigation of an ultrasonic spray atomiser used to pre-cool the air entering to the condenser of a heat pump used in air-conditioning applications. A set of 12 experimental tests were conducted on a test bench consisting of a subsonic wind tunnel with an ultrasonic spray atomiser installed in the test section. The influence of the air velocity and mass flow rate of sprayed water (depending on the number of active atomisers) on the performance of the system was investigated. The results of the study show the pre-cooling capacity of this system, under different operating conditions, through several performance indicators: evaporative cooling efficiency (saturation efficiency), temperature drop, wet bulb depression and evaporated water efficiency. The highest values of evaporative cooling efficiency occur in the low speed range of the tested airflows, for configurations of the atomisation system with a high number of active atomisers, and it has been found that the evaporative pre-cooling process is not homogeneous throughout the airflow for some operating conditions.

Keywords:

Evaporative cooling, ultrasonic spray atomiser, cooling efficiency, air conditioning

1. Introduction

Evaporative cooling techniques applied to the condenser of a refrigerating machine represent one of the most effective and immediately applicable solutions for improving the efficiency of domestic and commercial air conditioning systems worldwide. With these techniques it is possible to reduce significantly, mainly in countries with hot-dry climates, the energy demand and the high consumption peaks. Energy savings contribute to reducing the dependence on fossil fuel in any country and have a direct impact on its economic development and growth, as well as decreasing greenhouse gas emissions.

A considerable amount of studies in the literature show the benefits of pre-cooling techniques applied to different air conditioning systems. There are different strategies to reduce the temperature of the air entering the condenser. The most widely studied systems can be classified into: evaporative packings or pads and spray or mist generators. For direct evaporative coolers, Martínez et al. [1] investigated how different thicknesses of cooling pads influenced the energy performance of a split-type air-conditioner. They found that the highest increase of 10.6% in the overall coefficient of performance (COP) was achieved by a thickness of about 100 mm. The main drawback of pre-cooling systems based on evaporative pads is the additional pressure drop produced in the condenser air stream. Furthermore, this effect is present even if pre-cooling is not activated. Pressure drop causes a reduction in the air flow rate through the condenser and a decrease in its ability to reject heat to the environment. This means an increase in the condensation pressure, an additional compressor consumption and a reduced cooling capacity of the air-conditioning system, [2]. When water is sprayed over the evaporative pads and pre-cooling is activated, the temperature drop of the intake air to the condenser far outweighs both effects, the pressure drop and the air flow rate reduction, and results in savings of energy consumed by the compressor. However, when the water injection is not activated, the evaporative pads still generate a pressure loss that penalises the energy consumption in the compressor. Compared with direct evaporative coolers, mist or deluge systems give further installation flexibility because of their low profile piping network and provide negligible flow resistance to the air stream. Yu et al. [3] analysed the cooling effectiveness of mist in pre-cooling condenser air for an air-cooled chiller. In a subtropical climate, pre-cooling the condenser air by mist brought an increase of 0.36–8.86% and 0.34–10.19% in the coefficient of performance of the chiller

https://doi.org/10.52202/069564-0137

under the normal mode (conventional head pressure control) and the VSD mode (variable speed control for the condenser fans), respectively. However, the use of water spray or deluge can cause corrosion, scaling, and fouling on the heat exchanger bundles if water droplets are carried by the airstream to the heat exchanger bundles of the condenser. To avoid this, the system is required to evaporate all water in the airstream to prevent water droplet contact with the heat exchanger surface. Special wet media or spray nozzles may be required to meet the requirement. High-pressure nozzles provide small water droplets but at a higher cost. Water quality affects the performance of the nozzles and their maintenance cost, [4]. In view of the drawbacks found in current techniques for pre-cooling, a search for alternatives seems appropriate.

Applications of ultrasonic energy to enhance a wide variety of processes or to improve system efficiency have been explored in recent years. Yao [5] reviewed the studies addressing the applications of ultrasound as a new technology in the field of Heating, Ventilation and Air-Conditioning (HVAC). The author claimed that, from a general point of view, all the effects produced by ultrasound could be interesting in applications involving heat or mass transport, decreasing both the external and internal resistance to transport. Yao et al. [6] presented a review of the state-of-the-art of high-intensity ultrasound and its applications. However, the authors did not specifically cite evaporative cooling as an application of ultrasound, denoting the little attention they have received to date. Up to the knowledge of the authors, the studies conducted by Ruiz et al. [7] and Martinez et al. [8] were the first attempt to apply ultrasonic techniques (mist generator) to pre-cool the air entering the condenser in an air conditioning application. The authors experimentally analysed the performance of an ultrasonic mist generation system in [8]. Its thermal performance and its water mist production capacity were assessed in terms of the mass flow rate of atomised water and size distribution of the droplets generated. A CFD model of an ultrasonic mist generator specifically designed for HVAC applications was reported in [7]. The model was validated using the results obtained in [8], and the authors conducted a parametric analysis including some physical variables involved in the cooling process, and, finally, carried out an optimisation process regarding the overall cooling performance of the ultrasonic generator.

However, although the tests were satisfactory and their scientific interest has been revealed by the recent publications achieved, there are still many aspects related to the search for the optimal design of the pre-cooling system based on ultrasound techniques (reduce wet length and water power consumption). In conclusion, the works referring to the pre-cooling of the inlet air with ultrasonic atomisation techniques have been reviewed and it has been observed that this technique has received limited attention for this application, with few references found in the literature to date. Despite this, it has been proven that ultrasound technology constitute a promising method to improve the design of evaporative pre-cooling systems. Therefore, the main objective of this paper is to study the performance of an ultrasonic spray atomiser used to pre-cool the air entering to the condenser of a heat pump used in air-conditioning applications. The influence of the air velocity and mass flow rate of sprayed water (number of atomisers) on the performance of the system was investigated.

2. Materials and methods

2.1. Experimental test facility

To evaluate the performance and cooling capacity of the water mist produced by the ultrasonic atomiser, a set of tests has been conducted on a redesigned test bench specifically adapted for this purpose. The test rig mainly consists of two components: ultrasonic spray atomisers and a subsonic wind tunnel where evaporative cooling takes place.

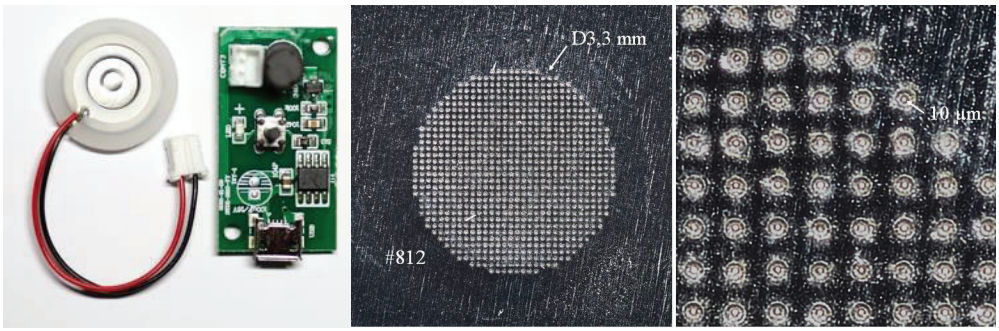

(a) (b)

Figure 1: (a) Used ultrasonic spray atomisers and an oscillator circuit PCB. (b) Microscopic image of the water outlet holes in the spray atomisers used.

https://doi.org/10.52202/069564-0137

The device used in the system is a ultrasound spray atomiser (Fig. 1 (a)). This is composed of a ceramic piezoelectric, which surrounds a porous metallic membrane, and an oscillator circuit PCB that generates a pulse signal at a frequency of 108 kHz for the spray atomiser. When the current is supplied, the piezoelectric initiates an expansion/contraction cycle. This oscillation allows the water to pass through its microscopic holes (around 10 μm, Fig. 1 (b)) , and pushes the drops forming a column of water spray. The mass flow rate is approximately $1.95 \cdot 10^{-5}$ kg s^{-1}. This component is characterised by having a low cost and consumption (1.3 W). Table 1 shows the operating conditions and technical specifications of a spray atomiser.

Table 1: Spray atomiser technical specifications.

Magnitude	Value
Disc diameter	15.5 mm
Ceramic core diameter	8.5 mm
Porous membrane diameter	3.3 mm
Microscopic Holes Diameter	10 μm
Input voltage	DC 5 V
Power	1.3 W
Resonance frequency	108 kHz
Mass flow rate	$1.95 \cdot 10^{-5}$ kg s^{-1}
Exit speed of the drops	2.5 m s^{-1}

In this research, several atomisers work at the same time, therefore, a hydraulic installation was built to supply several units at the same time. For this, an ABS plastic body was used for the connection of the atomisers with a system of flexible silicone pipes. On the other hand, to avoid creating bubbles in the pipes, it was decided to use a low-flow pump (RS PRO 20) for the recirculation of the water. It has a maximum flow rate of 650 ml min^{-1} and a consumption of 5 W. Fig. 2 shows a schematic representation of the configuration of 5 $\times$ 5 atomisers (rows $\times$ columns) with which the experimental tests were carried out.

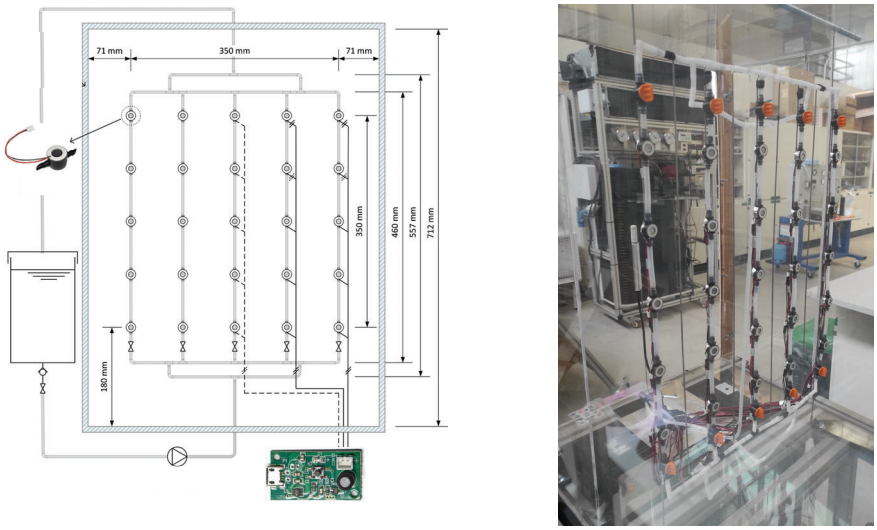

Figure 2: Scheme of the distribution of the spray atomisers in the form of a 5 $\times$ 5 manifold.

To carry out the experimental tests of ultrasonic evaporative cooling, the open-circuit subsonic wind tunnel shown in Fig. 3 was used. To ensure stable and uniform velocity profiles of the air flow, a nozzle was used along the honeycomb baffle (anti-turbulence screen), which was adapted for the tunnel entrance (leftmost part). It is not shown in the Fig. 3 because it is removed when modifications are made to the atomiser system. This nozzle has dimensions of 1.2 $\times$ 1.7 m^2 (cross-sectional) and a length of 1.55 m. While the test section of the wind tunnel has a cross section of 0.492 $\times$ 0.712 m^2 and a length of 5.3 m. A axial fan of 0.55-kW has been used to create the air flow inside the tunnel, which is located at the tunnel exit. This is associated with a variable-frequency drive that allows different air flows to be configured (from 0–3 m s^{-1}). The maximum

https://doi.org/10.52202/069564-0137

volumetric air flow rate allowed by the fan is 3783 m^3 h^{-1}. A detailed description of the wind tunnel can be found in [9,10].

Figure 3: Subsonic wind tunnel facility in which the experimental tests are carried out.

2.2. Experimental procedure

A number of tests have been carried out to evaluate the performance of the ultrasonic spray system. Firstly, the flow rate of atomised water that the system is able to supply as a function of the number of working ultrasonic transducers has been studied by means of a gravimetric measurement method. A photographic technique with digital image processing has also been used to determine the size, emission speed and distribution of the droplets generated in the atomisation process. Finally, the pre-cooling capacity of atomised water when sprayed into an air stream has been evaluated as a function of both air flow velocity and atomised water flow rate (depending on the number of atomisers).

In order to reproduce in the wind tunnel the real operating conditions of the atomisation system when used to pre-cool the inlet air to a condenser of a conventional split-type air-conditioning system, tests were carried out with four different air flow rates covering the usual range of flow rates of this type of equipment: 0.5 m s^{-1}, 1 m s^{-1}, 1.5 m s^{-1} and 2 m s^{-1}. Different flow rates of atomised water were used in the tests using three configurations of the ultrasonic atomisation system with 5, 15 and 25 active atomisers, respectively, in order to determine the performance of the system in terms of water consumption and taking into account the power consumption of the ultrasonic transducers. Counting the different configurations of the atomisation system and the air flow velocities established in the wind tunnel, a total of 12 tests were carried out.

For each test, dry bulb temperature and relative humidity were measured at various positions along the central axis of the wind tunnel, as can be seen in Fig. 4, which shows a schematic of the location of the different sensors installed in the wind tunnel. On the other hand, a set of nine thermo-hygrometers was used to record the temperature and relative humidity distribution in a measurement cross section. T_{ms} and ϕ_{ms} refer to the average temperature and relative humidity at the measurement section. Finally, a hot-wire anemometer was used to measure the airflow peak velocity (v_a) at the centre of the wind tunnel. By means of a calibration test of the air flow through the tunnel, an experimental correlation was obtained to determine the mean velocity and the volumetric flow rate from this central peak velocity.

Table 2 shows the technical specifications and accuracy of the test bench probes used in both the wind tunnel calibration tests and during the experimental characterization tests of the ultrasonic spray atomiser. All measurements were recorded with a Keysight DAQ970A data acquisition unit incorporating two Keysight DAQM901A 20-channel multiplexer modules.

In accordance with UNE-EN 13741 [11], steady-state conditions were maintained throughout the wind tunnel tests. A maximum variation of ± 0.2°C at each of the temperature probes during a continuous measurement recording period of 5 minutes was set as the steady-state criterion for the tests. The temperature of the water supplied to the atomisation system was maintained in the same range of variation. Before the start of each test, all the equipment and instrumentation is started up with a stabilisation period of at least 20 minutes during which measurements are taken to correct the zero error of the temperature and relative humidity probes. In order to guarantee the repeatability of the measurements, each test lasted approximately 40 minutes, during

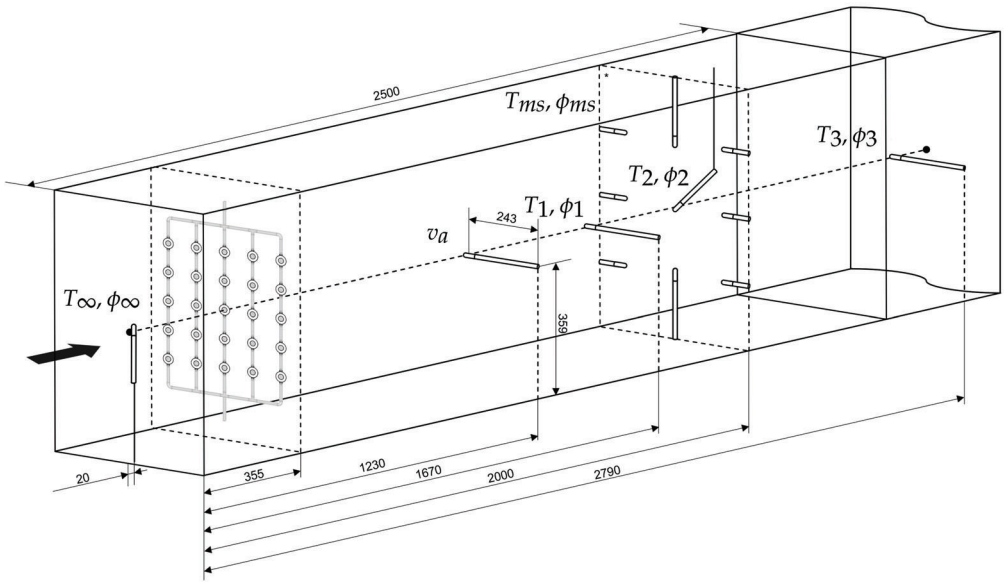

Figure 4: Schematic layout of the ultrasonic atomisation system and location of the probes and the measuring section in the wind tunnel.

Table 2: Specifications and characteristics of the test bench probes used during the experimental tests

Measurement	Measuring device	Brand	Model	Measuring range	Output signal	Accuracy
Air temperature	Thermohygrometer	E+E Elektronik	EE210-HT6xPBFxB	-20 to 80 °C	4–20 mA	± 0.2 °C
Air humidity	Thermohygrometer	E+E Elektronik	EE210-HT6xPBFxB	0–100% RH	4–20 mA	± (1.3+0.3% RD)% RH
Air temperature	Thermohygrometer	E+E Elektronik	EE210-HT6xPCxx	-20 to 80 °C	4–20 mA	± 0.2 °C
Air humidity	Thermohygrometer	E+E Elektronik	EE210-HT6xPCxx	0–100% RH	4–20 mA	± 2.5% RH
Air flow velocity	Anemometer	E+E Elektronik	EE65-VCD02	0–20 m/s	4–20 mA	± (0.2 m/s + 3% RD)
Air flow rate	Flow hood balometer	Testo	0563 4200	40–4000 m^3/h	USB port	± (12 m^3/h + 3% RD)
Power consump.	Power quality analyzer	Chauvin Arnoux	8334		USB port	± 1% RD
Water temperature	RTD-Pt100	Desin	ST-FFH PT100	-200 to 600°C	4-wires	± 0.05 °C
Water weight	Benchtop scale	PCE Instruments	PCE-TB 3	0–3 kg	4–20 mA	± 0.1 g

which measurements were taken every 7 seconds.

The atomised water flow rate was determined using a gravimetric method, measuring the initial and final mass of water supplied during each test with a benchtop scale and recording the time elapsed during the test. The average power consumption of the ultrasonic transducers was also determined by averaging the instantaneous power measured every 5 minutes.

3. Results and discussion

3.1. Measurement of water droplet size and spray emission speed

To determine the average size of the water droplets produced by the ultrasonic spray atomiser, a technique of high-speed photography and subsequent digital image processing has been used, similar to the method described by Ramisetty et al. [12]. A Pentax K-1 DSLR camera with a shutter speed of 1/8000s and a Tamron SP AF 90 mm F2.8 Di Macro 1:1 lens were used to measure the size of the droplets produced in the ultrasonic atomisation process. Due to the micrometric size of the droplets, it was necessary to attach an 18 cm extension tube to the lens to achieve a higher magnification of the captured images. The lighting was performed with a Pentax AF-360 FGZ automatic flash in TTL mode to achieve a t.5 peak duration time of approximately 1/20000 s.

Shots were taken over a reference atomiser, by placing the plume of atomised water between the lens and the flash and using a remote shutter release. The light emitted by the flash was filtered through a honey comb and then passed through a 3 mm grid to create a narrow illumination plane and thus reduce the number of drops that appear in each shot, as only the drops that cross the illumination plane are captured by the camera. An f-stop number of f/2.8 was used to provide a pronounced defocusing of the out-of-focus drops, so that some drops are isolated from others, which simplifies further digital processing.

https://doi.org/10.52202/069564-0137

The pictures taken with the camera were then processed with a graphic editor to increase contrast and acutance. An image analysis technique was used to measure the diameter of the droplets with both ImageJ and Fiji software. Fig. 5 shows an example of a high-speed shutter photography in which the movement of the droplets is frozen and diameter measurements can be made.

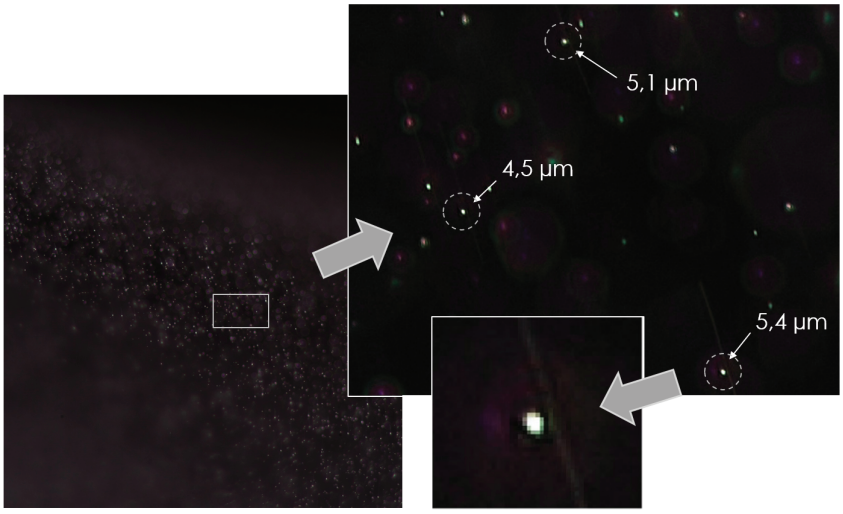

Figure 5: Example of a digitally processed high-speed photograph showing droplet diameter and size distribution.

The arithmetic mean diameter ($D_{1,0}$) and Sauter's mean diameter ($D_{3,2}$) of the droplets produced by the ultrasonic atomiser have been calculated according to the following general equation of the mean diameter:

$$D_{p,q} = \left[\frac{\sum_{i=1}^{N} n_i d_i^p}{\sum_{i=1}^{N} n_i d_i^q} \right]^{\frac{1}{p-q}} \tag{1}$$

where n_i stands for the number of droplets with a diameter d_i.

Finally, the arithmetic mean diameter of the droplets emitted by the ultrasonic atomiser under the test conditions is approximately $D_{1,0}$ = 5.0 μm and the Sauter mean diameter is $D_{3,2}$ = 5.2 μm. The uncertainty of this measurement method was calculated by considering a $\pm$1 pixel variation in the droplet diameter measurement by digital image processing. Taking into account the native camera resolution of 7360$\times$4912 pixels and the lens magnification factor, the maximum uncertainty was estimated to be $\pm$1.6 μm.

With this photographic technique it was also possible to measure the emission speed of the droplets generated in the ultrasonic atomisation process. From high-speed images showing the starting sequence of the atomised water injection (see Fig. 6), an approximate spray emission speed of 2.4 m s^{-1} was determined. This value is important to be able to perform a CFD simulation of the process and to determine the boundary conditions of the numerical model.

3.2. Thermal performance of the ultrasonic spray system

Table 3 summarises the operating conditions and configuration of the ultrasonic atomisation system in the conducted thermal performance tests and the experimental measurements obtained by the probes.

Based on the measurements obtained, a first study of the thermal behaviour of the atomisation system was carried out, taking into account the temperature drop reached in the air flow as it moves longitudinally through the wind tunnel. In this case, the temperature measurements obtained by the T_∞, T_1, T_2 and T_3 probes located on the central axis of the wind tunnel have been considered. A visual inspection of the water mist plume was also carried out during the tests to approximately determine the degree of evaporation of the supplied water flow, since as long as it is visible it indicates that there are still non-evaporated droplets that may be able to produce additional evaporative cooling within the air flow.

Fig. 7 shows the results of the longitudinal evolution of the temperature drop for the three configurations of 5, 15 and 25 active atomisers and for the different levels of air flow velocity considered in the tests. These graphs

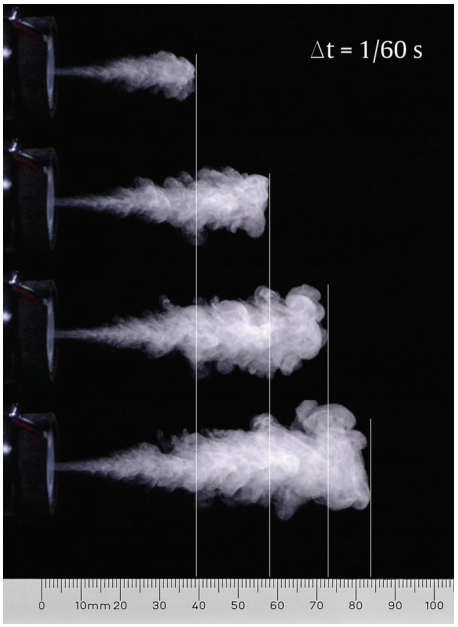

Figure 6: High-speed images showing the initial sequence of atomised water injection used to determine the spray emission speed.

Table 3: Summary of experimental tests of thermal performance on the ultrasonic atomisation system

Test run	config.	v_a (m s^{-1})	$\dot{m}_w$ (kg s^{-1})	T_∞ (°C)	ϕ_∞ (%)	T_1 (°C)	ϕ_1 (%)	T_2 (°C)	ϕ_2 (%)	T_{ms} (°C)	ϕ_{ms} (%)	T_3 (°C)	ϕ_3 (%)
1	5×1	0.5	9.8×10^{-5}	29.3	54.7	27.3	65.1	28.6	55.0	28.1	60.4	28.5	56.2
2	5×1	1.0	9.8×10^{-5}	28.8	47.3	27.9	50.5	28.0	47.4	28.3	48.7	27.9	48.9
3	5×1	1.5	9.8×10^{-5}	28.1	60.1	27.1	65.8	27.1	62.4	27.6	62.1	27.0	64.3
4	5×1	2.0	9.8×10^{-5}	28.8	57.0	28.0	61.0	28.0	58.2	28.4	58.4	27.9	59.5
5	5×3	0.5	2.9×10^{-4}	29.5	54.8	25.2	79.4	25.3	75.0	26.3	73.2	24.9	81.2
6	5×3	1.0	2.9×10^{-4}	28.7	49.4	26.9	57.7	26.8	55.4	27.2	56.4	26.5	57.3
7	5×3	1.5	2.9×10^{-4}	29.2	53.9	27.5	62.2	27.6	58.5	28.1	58.6	27.3	60.8
8	5×3	2.0	2.9×10^{-4}	29.6	53.0	28.3	58.8	28.3	55.7	28.6	56.7	27.9	58.7
9	5×5	0.5	4.9×10^{-4}	29.5	45.4	22.7	85.3	23.0	78.0	24.3	73.9	24.1	75.0
10	5×5	1.0	4.9×10^{-4}	30.9	36.3	26.3	55.4	26.2	52.5	28.5	44.1	26.8	50.4
11	5×5	1.5	4.9×10^{-4}	29.4	40.4	26.2	53.5	26.2	50.9	27.7	46.0	26.5	52.0
12	5×5	2.0	4.9×10^{-4}	29.2	40.7	26.8	50.6	26.7	47.7	27.9	44.7	26.8	50.2

show, as expected, that the largest temperature drops occur at lower levels of air velocity, since low velocity leads to an increase in the residence time of the water droplets in the air, which allows a higher transfer of sensible and latent heat between the water and the air.

For low air velocity levels (0.5–1 m s^{-1}), the largest longitudinal temperature drop occurs in almost all cases at probe T_1, the first one downstream of the atomisation section. From that moment on, the temperature drop of the air evolves along the tunnel, slightly decreasing its value. This effect is caused by the fact that the volume of atomised water is more concentrated at the centre of the tunnel and, therefore, this is where the evaporative cooling of the air is most intense, whereas at points away from the centre, the air temperature does not decrease as much. Far away from the atomisation section, a progressive temperature equilibrium is established in the air flow, which causes the temperature value measured at the central axis to be closer to the average temperature of the air flow cross-section at that location. The resulting non-homogeneity in the atomisation process is the reason for the longitudinal decrease in temperature drop observed in the graphs for the different levels of air velocity.

On the other hand, for higher air velocities (1.5–2 m s^{-1}) the highest temperature drop occurs at a distance further away from the atomisation section, between the probes T_1 and T_2, because at these velocities the droplets travel a longer distance before evaporating completely.

In the results for the configuration of 5 active atomisers, some anomalous behaviours are observed, such as a sharp drop in the temperature drop at the end of the tunnel for the velocity of 0.5 m s^{-1}. This may be due to

https://doi.org/10.52202/069564-0137

the lack of uniformity in the generation of atomised water, which is more pronounced the smaller the number of active atomisers.

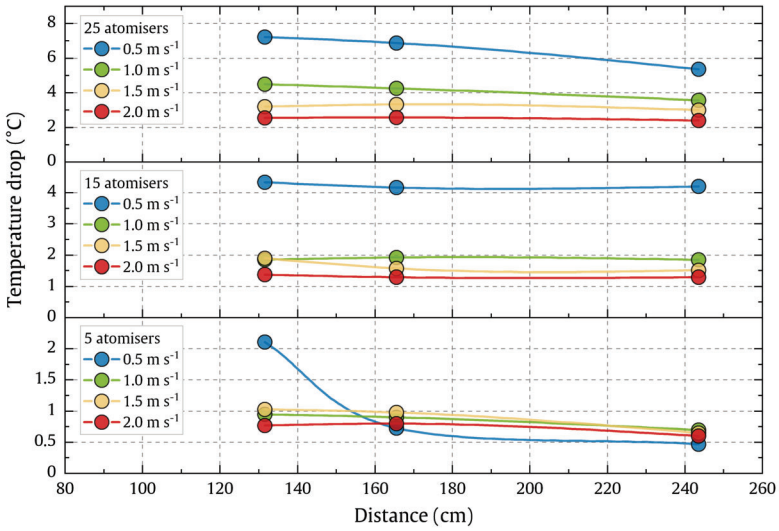

Figure 7: Temperature drop measured by the thermo-hygrometers located on the longitudinal axis of the wind tunnel, as a function of the distance of the probes from the atomisation section and the velocity of the air flow.

A study of the thermal behaviour of the atomisation system was then carried out, centred on a measurement cross-section in which a total of 9 thermo-hygrometers were installed to record the level of homogeneity of the evaporative cooling caused in the air flow. Table 4 and Fig. 8 show the values of the temperature drop recorded in each of the thermohygrometers that constitute the measurement section, for the three configurations of the atomisation system (5, 15 and 25 active atomisers) and for the four levels of air flow velocity.

Table 4: Temperature drop (°C) recorded on the 9 thermo-hygrometers located in the measuring cross-section of the wind tunnel, as a function of the active number of atomisers and the different levels of air flow velocity.

	Air flow velocity											
	0.5 m s^{-1}			1 m s^{-1}			1.5 m s^{-1}			2 m s^{-1}		
25 atomisers	1.0	3.8	2.8	1.6	0.8	2.3	0.9	0.4	1.2	0.9	0.3	1.3
	6.1	6.9	6.0	2.6	4.3	3.6	1.9	3.3	2.6	1.7	2.6	2.1
	6.4	7.2	6.5	1.6	3.6	2.1	0.8	2.1	0.9	0.6	1.6	1.0
15 atomisers	0.3	0.5	0.7	1.2	1.3	0.9	0.3	0.3	1.5	0.4	0.1	1.3
	3.8	4.2	4.8	2.0	1.9	2.1	1.1	1.6	1.9	0.9	1.3	1.4
	4.3	5.0	4.9	1.2	2.4	1.9	1.0	1.2	1.0	0.9	1.1	1.1
5 atomisers	0.2	0.1	0.4	0.5	0.4	0.2	0.2	0.1	0.1	0.4	0.1	0.2
	0.4	0.7	1.2	0.9	0.9	0.4	1.0	1.0	0.3	0.3	0.8	0.4
	2.7	2.7	2.9	0.7	1.7	0.3	0.3	0.9	0.4	0.3	1.1	0.5

From the temperature drop measurements, it can be seen that, for low velocities, very significant temperature drops are obtained in all the tests. However, as the number of active atomisers decreases, the temperature drop registered on the upper thermo-hygrometers and those located in the central area decreases. A lack of uniformity in the temperature drop can also be observed and, for example, the temperature drop in the upper right area of the measurement section is usually higher than that obtained in the upper left area. This situation may be caused by non-uniform atomisation of water or also by the development of turbulent vortices in the air flow. For all three configurations of the atomisation system, as the velocity increases, the temperature drop in the measurement section decreases, because the air mass flow rate is higher.

Fig. 9 shows a comparison of the calculated average values of the evaporative cooling efficiency or saturation efficiency (η_{sat}) and the wet bulb depression (WBD) for the three configurations of the atomisation system and

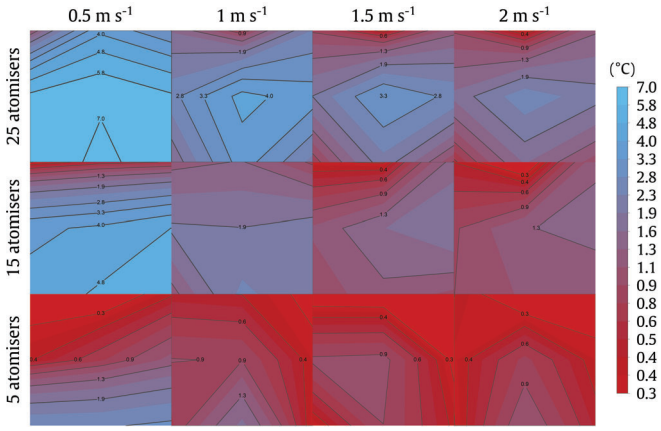

Figure 8: Contour plot of data presented in Table 4.

as a function of different air flow velocities. The saturation efficiency and the wet bulb depression have been calculated from the following expressions:

$$\eta_{sat} = \frac{\omega_{ms} - \omega_{\infty}}{\omega_s^* - \omega_{\infty}} = \frac{T_{\infty} - T_{ms}}{WBD} \tag{2}$$

$$WBD = T_{\infty} - T_{wb} \tag{3}$$

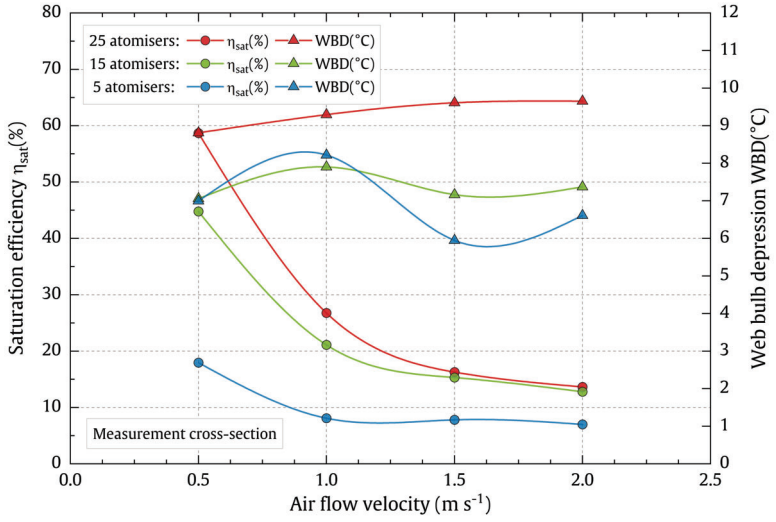

Figure 9: Comparison of the saturation efficiency (η_{sat}) and the wet bulb depression (WBD) for the three configurations of the atomisation system and as a function of different air flow velocities.

In Fig. 9 we can see that for high air flow velocities (1.5 m s^{-1} and 2 m s^{-1}) the results are very similar in the configurations of 25 and 15 atomisers. However, the saturation efficiency alone may be insufficient to obtain a clear interpretation of the evaporative cooling phenomenon taking place and it is necessary to include in the graph the wet bulb depression, which represents the largest possible temperature drop, i.e., the difference between the dry bulb temperature of the incoming air and its wet bulb temperature. Thus, if we compare the configurations of 15 and 25 atomisers for high air flow velocities we can see that, although they have a very similar saturation efficiency, as the web bulb depression is higher in the case of 25 atomisers, this implies that the temperature drop will also be higher for the configuration of 25 atomisers.

https://doi.org/10.52202/069564-0137

Finally, Fig. 10 shows a comparative study for the configuration of 25 atomisers of the evaporative cooling achieved in the measurement cross-section with respect to the maximum cooling that could be obtained if the entire flow of atomised water were evaporated before reaching the measurement cross-section. For this study, a novel performance indicator called evaporated water efficiency (η_{evap}) was considered, that denotes the extent to which the temperature in a particular region of the air flow (T_{ms}) approaches the minimum temperature (T_{min}) that would be reached if all the atomised water evaporates, defined as:

$$\eta_{evap} = \frac{T_\infty - T_{ms}}{T_\infty - T_{min}} = \frac{T_\infty - T_{ms}}{\frac{\dot{m}_w h_{fg}}{\dot{m}_a c_{pma}}} = \frac{1}{r_w} \frac{c_{pa} + \omega_a c_{pv}}{h_{fg}} (T_\infty - T_{ms}) \tag{4}$$

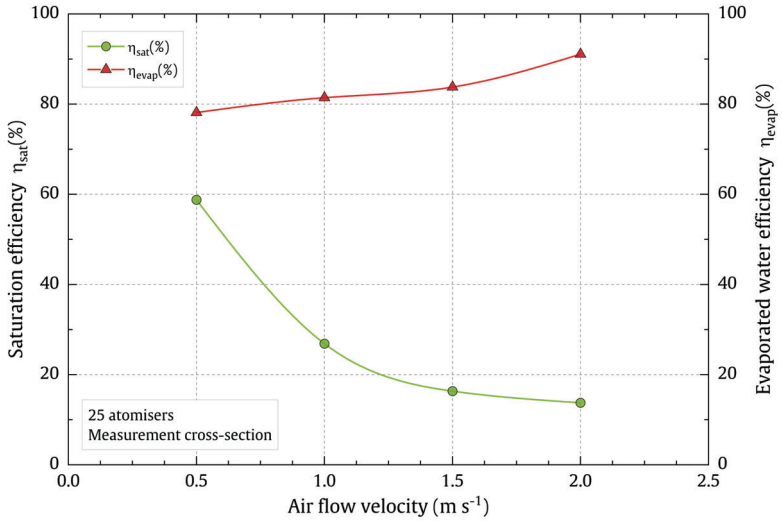

Figure 10: Comparative study of the saturation efficiency and the evaporated water efficiency for the configuration of 25 atomisers. Values close to η_{evap} = 100% indicate a more uniform distribution of the evaporative cooling effect.

The evaporated water efficiency can be used to identify the operating conditions of the atomisation system that lead to the most uniform and homogeneous evaporative cooling (η_{evap} = 100%) throughout the air flow, with complete utilisation of the supplied water.

4. Conclusions

In this article, an experimental study of the operating conditions and thermal behaviour of an ultrasonic atomisation system for evaporative pre-cooling of the inlet air of a condenser in air conditioning applications has been carried out.

Firstly, a measurement of the water droplet size and the emission speed of the atomiser was conducted using a high-speed photography technique and digital image processing to determine the average size of the water droplets produced by the ultrasonic atomiser and the emission speed of the atomiser. As a result, it has been obtained that the arithmetic mean diameter of the droplets emitted by the ultrasonic atomiser under the test conditions is approximately $D_{1,0}$ = 5.0 μm, the Sauter mean diameter is $D_{3,2}$ = 5.2 μm, and the approximate spray emission speed is 2.4 m s^{-1}.

An experimental study of the thermal behaviour of the atomisation system was then carried out in a wind tunnel to determine the longitudinal and transversal evolution of the temperature drop, specific humidity and saturation efficiency at different locations along the central axis of the wind tunnel and at a specific cross-section downstream of the atomisation section. The results of this study have provided information on the configurations of the atomisation system and the air flow velocities that provide the greatest potential of pre-cooling.

A maximum temperature drop of 7.2℃ was obtained for a configuration of 25 atomisers and 0.5 m s^{-1} at the temperature probe T_1, located at 131.5 cm from the atomisation section. Under the same operating con-

https://doi.org/10.52202/069564-0137

ditions, the maximum saturation efficiency, calculated from the 9 thermo-hygrometers in the measurement cross-section, was 58.7% and the wet bulb depression value was 8.8°C.

It has been noticed that the lowest air velocities lead to the highest saturation efficiencies in the measurement cross-section. Furthermore, it has been found that for velocities of 0.5 m s^{-1} and 1 m s^{-1}, and for a configuration of 25 atomisers, the supplied water is almost completely evaporated when the air flow reaches the measurement cross-section, located 164.5 cm downstream of the atomisation section.

Finally, it has been found that the evaporative cooling process is not homogeneous throughout the air flow under many operating conditions, so a new performance indicator called evaporated water efficiency (η_{evap}) has been defined to specifically evaluate this phenomenon.

From the results of this study, it is concluded that an ultrasonic atomisation system is a promising alternative to conventional evaporative cooling systems that can be used to pre-cool the incoming air flow into a condenser with the following advantages: no pressure loss in the air flow; no maintenance, cleaning or replacement of evaporative pads and no accumulation of salts; no recirculation or storage of a large volume of water. However, there are a number of issues that still need to be addressed in future research, such as optimising the energy consumption of the ultrasonic transducers and increasing the evaporation rate of the droplets to reduce the wet length and reduce the potential impact of droplets on the condenser heat exchanger. A final issue to be solved is the optimisation of the atomised water distribution to ensure a more homogeneous pre-cooling throughout the air flow.

Acknowledgments

The authors acknowledge the financial support received from the Government of Valencia (Generalitat Valenciana), through project AICO/2021/190 (Subvenciones para grupos de investigación consolidables).

Nomenclature

c_{pa} specific heat at constant pressure of dry air, J kg^{-1} K^{-1}

c_{pv} , specific heat at constant pressure of water vapour, J kg^{-1} K^{-1}

$D_{1,0}$, arithmetic mean diameter, m

$D_{3,2}$, Sauter mean diameter, m

h_{fg} , enthalpy of vaporization, J kg^{-1}

$\dot{m}_a$, inlet air mass flow rate at wind tunnel, kg s^{-1}

$\dot{m}_w$, mass flow rate of spray atomisers, kg s^{-1}

r_w , water mist to air mass flow ratio

T , dry bulb temperature, °C

T_{wb} , wet bulb temperature of moist air, °C

v_a , air flow velocity, m s^{-1}

Greek symbols

η_{evap} , evaporated water efficiency

η_{sat} , saturation efficiency

ω , humidity ratio of moist air, kg_w kg_a^{-1}

ω_s^* , humidity ratio of saturated moist air evaluated at T_{wb}, kg_w kg_a^{-1}

ϕ , relative humidity

Subscripts and superscripts

a air

∞ , ambient conditions

ma , moist air

https://doi.org/10.52202/069564-0137

ms , measurement section

v , water vapour

w , water

wb , wet bulb

Abbreviations

CFD , computational fluid dynamics

COP , coefficient of performance

PCB , printed circuit board

WBD , wet bulb depression

References

[1] Martínez P, Ruiz J, Cutillas CG, Martínez PJ, Kaiser AS, Lucas M. Experimental study on energy performance of a split air-conditioner by using variable thickness evaporative cooling pads coupled to the condenser. Applied Thermal Engineering. 2016;105:1041 1050. Available from: http://www.sciencedirect.com/science/article/pii/S1359431116300175.

[2] Mehrabi M, Yuill D. Generalized effects of faults on normalized performance variables of air conditioners and heat pumps. International Journal of Refrigeration. 2018;85:409 430. Available from: http://www.sciencedirect.com/science/article/pii/S0140700717304012.

[3] Yu FW, Ho WT, Chan KT, Sit RKY. Theoretical and experimental analyses of mist precooling for an air-cooled chiller. Applied Thermal Engineering. 2018;130:112 119. Available from: http://www.sciencedirect.com/science/article/pii/S1359431116321895.

[4] Hooman K, Guan Z, Gurgenci H. 9 - Advances in dry cooling for concentrating solar thermal (CST) power plants. In: Blanco MJ, Santigosa LR, editors. Advances in Concentrating Solar Thermal Research and Technology. Woodhead Publishing Series in Energy. Woodhead Publishing; 2017. p. 179 212. Available from: http://www.sciencedirect.com/science/article/pii/B9780081005163000095.

[5] Yao Y. Research and applications of ultrasound in HVAC field: A review. Renewable and Sustainable Energy Reviews. 2016;58:52 68. Available from: http://www.sciencedirect.com/science/article/pii/S1364032115016056.

[6] Yao Y, Pan Y, Liu S. Power ultrasound and its applications: A state-of-the-art review. Ultrasonics Sonochemistry. 2020;62:104722. Available from: http://www.sciencedirect.com/science/article/pii/S1350417719308995.

[7] Ruiz J, Martínez P, Martín I, Lucas M. Numerical Characterization of an Ultrasonic Mist Generator as an Evaporative Cooler. Energies. 2020;13(11). Available from: https://www.mdpi.com/1996-1073/13/11/2971.

[8] Martínez P, Ruiz J, Íñigo Martín, Lucas M. Experimental study of an ultrasonic mist generator as an evaporative cooler. Applied Thermal Engineering. 2020;181:116057. Available from: https://www.sciencedirect.com/science/article/pii/S1359431120335377.

[9] Martínez P, Ruiz J, Martínez PJ, Kaiser AS, Lucas M. Experimental study of the energy and exergy performance of a plastic mesh evaporative pad used in air conditioning applications. Applied Thermal Engineering. 2018;138:675 685. Available from: http://www.sciencedirect.com/science/article/pii/S1359431117378225.

[10] Ruiz J, Cutillas CG, Kaiser AS, Zamora B, Sadafi H, Lucas M. Experimental study on pressure loss and collection efficiency of drift eliminators. Applied Thermal Engineering. 2019;149:94 104. Available from: http://www.sciencedirect.com/science/article/pii/S1359431118355388.

[11] UNE-EN 13741:2004 Thermal performance acceptance testing of mechanical draught series wet cooling towers. Spanish Standardization; 2004.

[12] Ramisetty K, Pandit A, Gogate P. Investigations into ultrasound induced atomization. Ultrasonics sonochemistry. 2012 05;20:254-64.